

Conformational Stability of 3-Fluoropropene in Rare Gas Solutions from Temperature-Dependent FT-IR Spectra and *ab Initio* Calculations

B. J. van der Veken and W. A. Herrebout

Rijksuniversitair Centrum Antwerpen, Laboratorium voor Anorganische Scheikunde, Groenenborgerlaan 171, 2020 Antwerpen, Belgium

D. T. Durig,[†] Wayne Zhao, and J. R. Durig*

Department of Chemistry, University of Missouri–Kansas City, Kansas City, Missouri 64110-2499

Received: August 25, 1998; In Final Form: January 8, 1999

The infrared spectra (3500–400 cm^{-1}) of 3-fluoropropene (allyl fluoride), $\text{CH}_2=\text{C}(\text{H})\text{CH}_2\text{F}$, dissolved in liquid argon, krypton, and xenon have been recorded at various temperatures ranging from -180 to -65 °C. From these studies, the enthalpy difference between the more stable *cis* conformer and the high-energy *gauche* rotamer has been determined to range from 60 ± 8 cm^{-1} (718 ± 96 J/mol) in liquid xenon to 81 ± 1 cm^{-1} (969 ± 12 J/mol) in liquid argon. These values have been extrapolated utilizing a linear relationship between the Kirkwood function of the solvent and the enthalpy differences in the solvents to give a value of 130 ± 25 cm^{-1} (1.56 ± 0.30 kJ/mol) for the vapor. From the experimental enthalpy value, the *gauche* dihedral angle, torsional transitions for both rotamers, and better structural parameters, the potential function governing the conformational interchange has been recalculated. *Ab initio* calculations utilizing the 6-31G(d,p) and 6-311G(d,p) basis sets with electron correlation at the MP2 level predict the *cis* conformer to be the more stable rotamer, but from the MP2/6-311++G(d,p) calculation the *gauche* conformer is predicted to be more stable by 117 cm^{-1} (1.40 kJ/mol). By combination of the *ab initio* predictions of the structural parameters with the previously reported microwave rotational constants for 11 different isotopic species of both conformers, complete r_0 parameters have been obtained for both rotamers. The results of these structural parameter determinations are compared to those previously reported.

Introduction

The 3-fluoropropene molecule has been the subject of several spectroscopic studies for 2 decades, including infrared, Raman, microwave, and NMR spectroscopies.^{1–11} A number of studies have been devoted to its structure and thermodynamic stabilities. It has been shown that 3-fluoropropene exists as a mixture of *cis* and *gauche* rotamers with the *cis* conformer being the thermodynamically preferred form in the gas phase at ambient temperature. The enthalpy difference, ΔH , between the *cis* and *gauche* conformers has been determined experimentally in different phases by different techniques. From microwave relative intensity measurements¹ the enthalpy difference was determined to be 58 ± 23 cm^{-1} (694 ± 275 J/mol) with the *cis* rotamer the more stable form. In a subsequent microwave and far-infrared spectroscopic study² this value of the enthalpy was used, along with the torsional transitions, to obtain the potential function governing conformational interchange. A study⁴ of the temperature-dependent Raman spectrum of the vapor gave an enthalpy difference of 263 ± 25 cm^{-1} (3.15 ± 0.30 kJ/mol), again with the *cis* conformer the more stable form. This value was about 4 times larger than the value of 58 ± 10 cm^{-1} (694 ± 120 J/mol) obtained for the liquid.⁴

More recently, the energy difference of 211 ± 25 cm^{-1} (2.52 ± 0.30 kJ/mol) was obtained from a matrix isolation study⁸

TABLE 1: Experimental and Theoretical Values of the Energy Difference (cm^{-1}) between the Conformers of 3-Fluoropropene

method	state	ΔH (ΔE)	ref
Raman	liquid	58 ± 10	4
microwave	vapor	58 ± 23	1
microwave/far-infrared	vapor	108	2
Raman	vapor	263 ± 25	4
infrared matrix	vapor	211 ± 25	8
RHF/STO-3G		143	5
RHF/6-31G(d)		148	5
RHF/6-31G(d,p)		171	8
MP2/4-31G		216	8
MP4/4-31G//MP2/4-31G		276	8
MP2/6-31G(d,p)		256	8
MP4/6-31G(d,p)//MP2/6-31G(d,p)		266	8

assuming that the gas-phase equilibrium between the conformers is trapped upon deposition. Therefore, the experimental value of ΔH for the vapor phase ranges from 58 ± 23 to 263 ± 25 cm^{-1} , and it is clear from these data that the experimental value of ΔH for 3-fluoropropene is still relatively uncertain (Table 1). The energy difference between the two conformers of 3-fluoropropene has been obtained from *ab initio* calculations at various levels of theory. The values obtained are also listed in Table 1 and range from a low value of 143 cm^{-1} to a high value of 276 cm^{-1} , all with the *cis* conformer the more stable rotamer.

Considering the well-known advantages of low-temperature spectroscopy and the advantages of the spectroscopic studies

* Corresponding author. Phone: 01 816-235-1136. Fax: 01 816-235-5191. E-mail: durigj@umkc.edu.

[†] Studies carried out while on sabbatical leave from the Departments of Chemistry and Physics, The University of the South, Seawee, TN 37383.

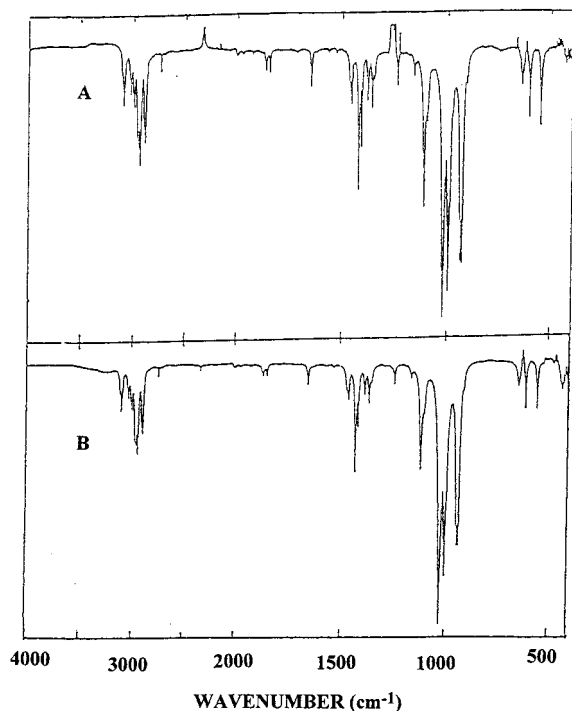


Figure 1. Infrared spectra of 3-fluoropropene in liquified noble gases: (A) in Kr and (B) in Xe.

of cryosolutions over the conventional solid matrix-isolation technique,¹¹ we have carried out variable temperature infrared spectroscopic studies of 3-fluoropropene in several liquified noble gases. Additionally, as previously pointed out,¹⁰ there exist artifacts in the experimentally determined structural data. Therefore, *ab initio* calculations employing larger basis sets with full electron correlation by the perturbation method¹² to second-order Moller–Plesset (MP2) have been performed, with particular attention to the ΔH values between the conformers along with the predicted structural parameters. It was expected that the present study could provide a more definitive value for ΔH of the vapor and better insight into the structural parameters for the two conformers of 3-fluoropropene. Both the theoretical and experimental results are reported herein.

Experimental Method

The sample of 3-fluoropropene was prepared by the reaction of 3-bromopropene with potassium fluoride in ethylene glycol in the manner previously described.¹³ Purification was carried out by a low-temperature, low-pressure fractionation column. The purity of the sample was checked by comparing the mid-infrared spectrum of the vapor with the previously reported spectrum.⁴

The mid-infrared spectra (Figure 1) of the sample dissolved in liquified noble gases (Ar, Kr, and Xe) as a function of temperature were recorded on a Bruker model IFS-66 Fourier transform interferometer equipped with a Globar source, a Ge/KBr beam splitter, and a TGS detector. High-purity noble gases (Matheson, 99.995%) were used typically in ca. (500–3000)-fold excess. The temperature studies, ranging from -65 to -180 °C with an accuracy of ± 0.3 °C, were performed in a specially designed cryostat cell that consisted of a 4 cm path length copper cell with wedged silicon windows sealed to the cell with indium gaskets and attached to a pressure manifold to allow for the filling and evacuation of the cell. The temperature was monitored with two Pt thermoresistors, while the cell was cooled

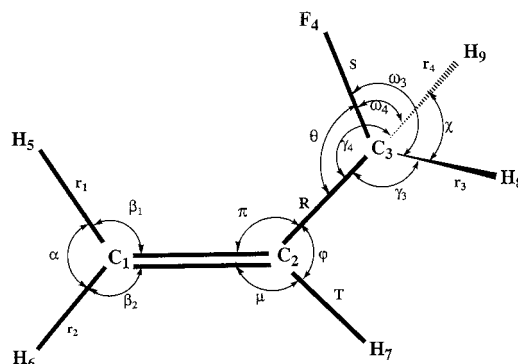


Figure 2. Atomic numbering and internal coordinates of 3-fluoropropene.

with boiling liquid nitrogen. Once the cell is cooled to the desired temperature, a small amount of sample is condensed into the cell. The cell is then pressurized with the noble gas, allowing the compound to dissolve. For each temperature investigated 200 interferograms were collected at 0.5 cm^{-1} resolution, averaged, and transformed with a Happ–Genzel apodization function. The frequencies obtained for the fundamentals for the *cis* and *gauche* conformers in the three different liquified noble gases are listed in Tables 2 and 3, respectively.

Computational Methodology

Complete geometric optimizations of the *cis* and *gauche* conformers of 3-fluoropropene were carried out using the Gaussian-94 program¹⁴ up to the MP2/6-311++G(d,p) level of calculation. The atomic numbering for this molecule is shown in Figure 2. The energy minima with respect to the nuclear coordinations were obtained by the simultaneous relaxation of all the geometric parameters using the gradient method of Pulay.¹⁵ The energies for the potential surface were obtained with optimization at 30° increments for fixed dihedral angles between 0° (*cis*) and 180° (*trans*). The transition states were characterized by one imaginary frequency. The vibrational frequencies were calculated by the classic Wilson GF matrix method¹⁶ with the different basis sets and levels. Subsequently, the scaled quantum mechanical force field was used to correct existing systematic errors for computed vibrational frequencies.

Infrared and Raman spectra were calculated using frequencies, infrared intensities, and Raman scattering activities determined from the MP2/6-311G(d,p) and RHF/6-311G(d,p) calculations, respectively. Infrared intensities were calculated on the basis of the dipole moment derivatives with respect to the Cartesian coordinates. The derivatives were taken from the *ab initio* calculations transformed to normal coordinates by

$$\left(\frac{\partial \mu_u}{\partial Q_i}\right) = \sum_j \left(\frac{\partial \mu_u}{\partial X_j}\right) L_{ij}$$

where the Q_i is the i th normal coordinate, X_j is the j th Cartesian displacement coordinate, and L_{ij} is the transformation matrix between the Cartesian displacement coordinates and normal coordinates. The infrared intensities were calculated by

$$I_i = \frac{N\pi}{3c^2} \left[\left(\frac{\partial \mu_x}{\partial Q_i}\right)^2 + \left(\frac{\partial \mu_y}{\partial Q_i}\right)^2 + \left(\frac{\partial \mu_z}{\partial Q_i}\right)^2 \right]$$

The Raman scattering cross section, $\partial \sigma / \partial \Omega$, which is proportional to the Raman intensity, can be calculated from the

TABLE 2: Observed and Calculated Vibrational Frequencies (cm⁻¹) for *cis*-3-Fluoropropene

species	ν_i	description	ab initio					observed liquid noble gases ^e					PED	
			MP2/6-311G-(d,p)	MP2/6-311++G-(d,p)	fixed scaled ^a	IR intens ^b	Raman act. ^c	gas ^d	Ar	Kr	Xe	liq ^d		solid ^d
A'	ν_1	=CH ₂ antisymmetric stretch	3307	3302	3138	4.2	54.9	3114	3111	3108	3104	3096	3108	99S ₁
	ν_2	=CH ₂ symmetric stretch	3211	3206	3046	5.4	154.8	3032	3029	3026	3023	3029	3026	37S ₂ , 62S ₃
	ν_3	=CH stretch	3196	3192	3032	6.8	30.9	2998	3005	3002	2998	2994	2998	62S ₂ , 37S ₃
	ν_4	-CH ₂ symmetric stretch	3087	3091	2928	36.9	156.5	2938	2941	2937	2933	2948	2945	100S ₄
	ν_5	C=C stretch	1713	1706	1625	2.4	37.0	1653	1654	1654	1654	1651	1649	69S ₅ , 12S ₇ , 8S ₉ , 7S ₁₂
	ν_6	-CH ₂ deformation	1531	1520	1452	3.1	12.5	1468	1470	1469	1467	1463	1461	95S ₆ , 55S ₈
	ν_7	=CH ₂ deformation	1461	1460	1386	11.6	7.6	1417	1414	1412	1412	1417	1416	57S ₇ , 19S ₈ , 11S ₁₂
	ν_8	-CH ₂ wagging	1443	1436	1369	10.1	4.1	1389	1385	1384	1383	1387	1385	65S ₈ , 25S ₇
	ν_9	=CH in-plane bending	1313	1313	1246	0.1	22.3	1292				1292	1284	60S ₉ , 15S ₁₀ , 16S ₅
	ν_{10}	CF stretch	1159	1145	1100	52.2	2.3	1118	1115	1114	1112	1108	1109	58S ₁₀ , 10S ₁₀ , 10S ₁₂ , 6S ₁₃
	ν_{11}	=CH ₂ wagging	1020	1015	968	28.8	5.0	971	971	970	970	973	976	53S ₁₁ , 15S ₉ , 28S ₁₁
	ν_{12}	C-C stretch	932	927	884	2.3	7.2	905	903	902	901	903	900	66S ₁₂ , 8S ₃ , 6S ₁₄
	ν_{13}	C-C-F bending	614	611	582	5.8	1.8	604	604	604	603	602	604	44S ₁₃ , 15S ₁₀ , 31S ₁₄
	ν_{14}	C=C-C bending	277	271	263	2.7	1.4	268				272	284	55S ₁₄ , 42S ₁₃
A''	ν_{15}	-CH ₂ antisymmetric stretch	3139	3143	2978	30.6	88.5	2960	2965	2962	2958	2960	2959	100S ₁₅
	ν_{16}	-CH ₂ twisting	1293	1283	1227	0.2	7.3	1253			1256	1244	1246	91S ₁₆ , 8S ₁₉
	ν_{17}	-CH ₂ rocking	1058	1050	1003	15.0	2.9	1032	1023	1022	1020	1020	1024	77S ₁₇ , 6S ₁₆ , 14S ₁₇
	ν_{18}	=CH out-of-plane bending	1026	1015	974	16.6	0.1	996	993	992	990	997	997	57S ₁₈ , 46S ₂₀
	ν_{19}	=CH ₂ out-of-plane bending	924	888	877	38.3	2.9	928	926	925	923		928	100S ₁₉
	ν_{20}	=CH ₂ twisting	556	546	527	9.1	7.2	549	560	550	549	555	567	60S ₂₀ , 29S ₁₇ , 12S ₁₉
	ν_{21}	asymmetric torsion	173	149	173	2.9	4.2	164					222	100S ₂₁

^a Calculated using the MP2/6-311G(d,p) level and scaled with scaling factors of 0.9 for stretches and bends and 1.0 for the torsion. ^b Infrared calculated intensities in km mol⁻¹ from MP2/6-311G(d,p) calculation. ^c Raman scattering activity in Å⁴ u⁻¹ from RHF/6-311G(d,p) calculation. ^d Reference 5. ^e This study.

TABLE 3: Observed and Calculated Vibrational Frequencies (cm⁻¹) for *gauche*-3-Fluoropropene

species	ν_i	no. ^a	description	ab initio					observed liquified noble gases ^f					PED	
				MP2/6-311G**	MP2/6-311++G**	fixed scaled ^b	IR intens ^c	Raman act. ^d	gas ^e	Ar	Kr	Xe	liq ^e		
A	ν_1	1	-CH ₂ antisymmetric stretch	3287	3285	3119	10.2	62.8	3100	3097	3094	3090	3096	97S ₁	
	ν_2	3	=CH stretch	3213	3212	3048	6.0	110.6	3008	3034	3030	3027	3015	93S ₂	
	ν_3	2	=CH ₂ symmetric stretch	3186	3184	3023	7.2	70.2		2995	2992	2989		95S ₃	
	ν_4	15	CH ₂ antisymmetric stretch	3159	3165	2997	26.3	63.0		2965	2962	2958	2960	97S ₁₅	
	ν_5	4	CH ₂ symmetric stretch	3096	3102	2937	35.9	116.8	2938	2901	2898	2894		99S ₄	
	ν_6	5	C=C stretch	1709	1701	1621	0.4	36.5	1646		1630	1628		68S ₅ , 13S ₇ , 8S ₉	
	ν_7	6	-CH ₂ deformation	1528	1522	1450	1.2	5.5		1462	1460	1458		98S ₆	
	ν_8	7	=CH ₂ deformation	1479	1475	1403	26.4	7.4	1432	1429	1428	1425	1428		58S ₇ , 26S ₈ , 8S ₉ , 6S ₁₂
	ν_9	8	-CH ₂ wagging	1423	1414	1350	11.3	5.8	1368	1364	1363	1362	1367		68S ₈ , 23S ₇
	ν_{10}	9	=CH in-plane bending	1313	1315	1246	0.2	17.1		1242	1240	1240			59S ₉ , 15S ₅ , 13S ₁₀
	ν_{11}	16	-CH ₂ twist	1298	1291	1231	3.6	11.7	1243				1244		83S ₁₆
	ν_{12}	12	C-C stretch	1197	1198	1136	5.5	1.8	1160	1098	1097	1096			25S ₁₂ , 11S ₉ , 18S ₁₁ , 11S ₁₃ , 30S ₁₉
	ν_{13}	10	C-F stretch	1089	1057	1033	104.7	5.2		1022	1022	1021			90S ₁₀
	ν_{14}	18	=CH out-of-plane bending	1029	1019	976	36.3	3.4		993	992	990			77S ₁₈ , 22S ₂₀
	ν_{15}	17	-CH ₂ rocking	1003	999	951	7.0	2.1		918	917		918		25S ₁₂ , 39S ₁₇ , 16S ₂₀
	ν_{16}	19	=CH ₂ out-of-plane bending	939	937	891	30.4	2.2		936	935	934			16S ₁₁ , 77S ₁₉
	ν_{17}	11	=CH ₂ wagging	934	918	886	6.8	3.3							39S ₁₁ , 12S ₁₂ , 29S ₁₉
	ν_{18}	20	=CH ₂ twist	657	656	622	6.9	4.7	641	640	640	638	644		14S ₁₂ , 16S ₁₈ , 55S ₂₀
	ν_{19}	13	C=C-C bending	438	435	416	2.4	4.3	422				438		51S ₁₄ , 20S ₁₃
	ν_{20}	14	C-C-F bending	334	339	317	6.5	2.7	332						49S ₁₃ , 32S ₁₄ , 6S ₁₇ , 9S ₂₀
	ν_{21}	21	asymmetric torsion	114	115	114	1.1	6.5	108						100S ₂₁

^a Vibrational quantum number of the equivalent vibration for the *cis* conformer. ^b Calculated using the MP2/6-311G(d,p) level and scaled with scaling factors of 0.9 for stretches and bends and 1.0 for the torsion. ^c Infrared calculated intensities in km mol⁻¹ from MP2/6-311G(d,p) level. ^d Raman Scattering activity in Å⁴ u⁻¹ from RHF/6-311G(d,p) level. ^e Reference 5. ^f This study.

scattering activities and the predicted frequencies for each normal mode using the relationship¹⁸⁻²¹

$$\frac{\partial \sigma_j}{\partial \Omega} = \left(\frac{2^4 \pi^4}{45} \right) \left(\frac{(\nu_0 - \nu_j)^4}{1 - \exp\left[\frac{-h\nu_j}{kT}\right]} \right) \left(\frac{h}{8\pi^2 c \nu_j} \right) S_j$$

where ν_0 is the exciting frequency, ν_j is the vibrational frequency of the *j*th normal mode, and S_j is the corresponding Raman scattering activity. To obtain the polarized Raman scattering

cross sections, the polarizabilities are incorporated into S_j by $S_j[(1 - \rho_j)/(1 + \rho_j)]$ where ρ_j is the depolarization ratio of the *j*th normal mode. The Raman scattering cross sections and calculated frequencies, together with a Lorentzian function, were used to obtain the calculated spectrum. Since the calculated frequencies are approximately 10% higher than those observed, the scaled quantum mechanical force fields were employed for corrections. The simulated infrared and Raman spectra for each conformer and their mixtures are shown in Figures 3 and 4, respectively. These spectra can be compared to the experimental

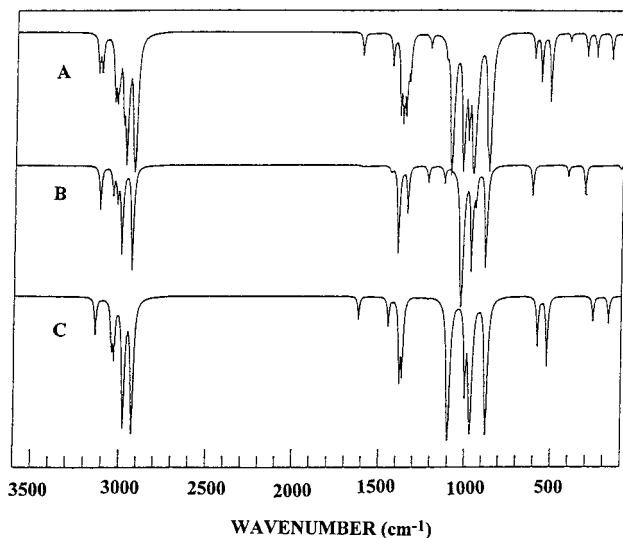


Figure 3. Calculated infrared spectra of 3-fluoropropene: (A) mixture of the cis and gauche conformers; (B) pure gauche; (C) pure cis.

spectra, and they provide support for the assignment of the observed bands to the indicated fundamentals, as well as for the enthalpy difference between the two conformers.

Structural Parameters

The optimized structural parameters and rotational constants with different basis sets for each conformer are listed in Tables 4 and 5, respectively, along with previously reported r_s and refined r_o structures. In comparing the computed results with experimental values, it is clear that a significant improvement has been reached when the ab initio calculations were performed with the larger basis sets at the MP2 level. The computed structural parameters at the MP2 levels give more realistic results, particularly for the C=C, C-F, and C-H bond distances than the RHF calculations. The C=C bond length calculated with the largest basis set at the MP2 level, i.e., MP2/6-311++G(d,p), are 1.3376 and 1.3393 for the cis and gauche conformers, respectively, which are about 0.005 Å longer than the r_s and r_o distances for these parameters even though they are r_e values. The remaining calculated parameters are in quite good agreement with the reported r_o parameters. The C-C bond (r_o) in the cis form is slightly longer by 0.005 Å than the corresponding distance in the gauche form that is predicted by the ab initio calculations. These results are sharply different from the previously reported¹ r_s values in which the gauche form was predicted to have two C-H distances more than 0.029 Å longer than the corresponding distance for the cis form, although the uncertainties for these parameters for the gauche conformer were nearly this large. For the C-H bond distances, the present results indicate that the C-H bonds on the vinyl group have similar bond lengths, which was not true for the r_s parameters. In general, calculated carbon-hydrogen bond lengths for both conformers have approximately the same values. The difference between them is less than 0.001 Å, except for the C₁-H₅ bond, which is predicted to be 0.0025 Å longer in the gauche form. Comparing the calculated C-F bond length to the corresponding r_o values, this bond in the gauche form deviates 0.005 Å from the r_o structure. It is probable that the C-F distances should differ between the two conformers by 0.008 Å, which suggests that the r_o C-F distance in the gauche form should be longer.

A striking difference for the structural parameters between conformers is found for both the \angle C-C-F and \angle C=C-C angles. Ab initio calculations predict that both angles in the cis

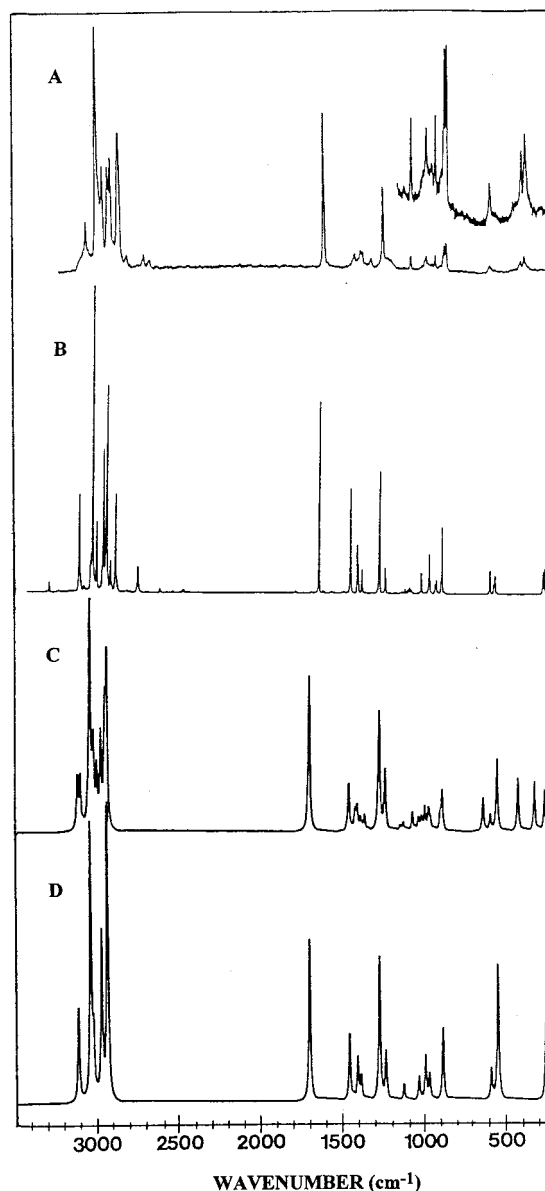


Figure 4. Comparison of experimental and calculated Raman spectra of 3-fluoropropene: (A) gas; (B) solid; (C) calculated mixture of cis and gauche conformers; (D) calculated pure cis form.

form are ca. 1.7° larger than the corresponding ones in the gauche form. The r_o values differ by only about 1.0°, but the larger r_o values for these two parameters for the gauche form compared to the ab initio values undoubtedly depends on the dihedral angle for the gauche conformer as well as on the C-F distance. In conclusion, the ab initio predicted parameters show little difference between conformers and give the closest agreement between the r_o values and ab initio structures from the MP2/6-311G(d,p) and MP2/6-311++G(d,p) calculations, with the former ones in better agreement with the microwave rotational constants.

Conformational Stability

With the availability of the liquified noble gases technique, the enthalpy difference between the two conformers of 3-fluoropropene was determined. The mid-infrared spectra of the sample dissolved in liquified krypton and xenon are shown in Figure 1. Because only small interactions are expected to occur between the dissolved molecules and the surrounding noble gas atoms,^{11,22-24} these "pseudo-gas-phase" spectra show only small

TABLE 4: Comparison of Computed and Experimental Structural Parameters for *cis*-3-Fluoropropene^a

parameter	MP2/6-31 G(d)	MP2/6-31 G(d,p) ^b	RHF/ 6-311G(d,p)	MP2/ 6-311G(d,p)	RHF/ 6-311++G(d,p)	MP2/ 6-311++G(d,p)	r_s^c	r_0^d	microwave adjusted ^e
$r(C_1=C_2)$	1.334	1.334	1.315	1.3357	1.3171	1.3378	1.333 ± 0.007	1.333 ± 0.003	1.333
$r(C_2-C_3)$	1.494	1.493	1.496	1.4960	1.4965	1.4955	1.503 ± 0.010	1.495 ± 0.004	1.494
$r(C_3-F)$	1.393	1.392	1.365	1.3833	1.3657	1.3886	1.382 ± 0.010	1.388 ± 0.004	1.390
$r(C_1-H_5)$	1.083	1.078	1.0746	1.0832	1.0749	1.0837	1.077 ± 0.007	1.083 ± 0.002	1.087
$r(C_1-H_6)$	1.084	1.079	1.0754	1.0837	1.0754	1.0839	1.106 ± 0.007	1.084 (fixed)	1.087
$r(C_2-H_7)$	1.089	1.083	1.0792	1.0883	1.0794	1.0886	1.090 assumed	1.089 (fixed)	1.092
$r(C_3-H_8)$	1.096	1.092	1.0848	1.0951	1.0848	1.0948	1.098 ± 0.007	1.098 ± 0.002	1.100
$r(C_3-H_9)$	1.096	1.092	1.0848	1.0951	1.0848	1.0948	1.098 ± 0.007	1.098 ± 0.002	1.100
$\angle C_1C_2C_3$	123.7	123.5	125.0	123.9	125.4	124.5	124.6 ± 0.8	124.5 ± 0.3	123.6
$\angle C_2C_3F$	111.0	111.0	111.5	111.6	111.6	111.5	111.7 ± 0.7	111.5 ± 0.3	112.4
$\angle C_2C_1H_5$	121.1	120.8	121.5	120.8	121.6	121.1	120.9 ± 0.5	121.1 ± 0.2	120.7
$\angle C_2C_1H_6$	121.3	121.2	121.0	121.0	120.9	120.7	119.2 ± 0.5	121.3 ± 0.2	119.6
$\angle H_5C_1H_6$	117.6	118.0	117.5	118.2	117.5	118.2	119.9 ± 0.5	117.6 ± 0.2	119.7
$\angle C_1C_2H_7$	120.9	120.9	120.5	120.7	120.4	120.5	119.0 assumed	120.9 ± 0.2	122.6
$\angle C_2C_3H_8$	111.0	110.8	110.6	110.4	110.7	110.7	111.1 ± 0.5	111.1 ± 0.3	111.7
$\angle C_2C_3H_9$	111.0	110.8	110.6	110.4	110.7	110.7	111.1 ± 0.5	111.1 ± 0.3	111.7
$\angle H_8C_3H_9$	108.0	108.6	108.5	108.5	108.5	108.6	108.1 ± 0.5	108.2 ± 0.2	107.4
$\angle H_8C_3F$	107.9	108.0	107.8	108.0	107.6	107.6	107.4 ± 0.5	107.9 ± 0.2	106.7
$\angle H_9C_3F$	107.9	108.0	107.8	108.0	107.6	107.6	107.4 ± 0.5	107.9 ± 0.2	106.7
dihedral	0.0	0.0	0.0	0.0	0.0	0.0	0.0	0.0	0.0
angle, φ									
A	17020		17107	17218	17818	17210	17400	17234	17238
B	6092		6133	6043	6002	5997	5941	6007	6003
C	4616		4622	4602	4618	4576	4556	4582	4580
$-(E + 215)$ (hartree)		1.524771	0.978871	1.684670	0.983840	1.694874			
ΔE (cm ⁻¹)			-174	-191	-19	117			

^a Bond lengths in angstroms; angles in degrees; rotational constants in MHz. ^b Reference 8. ^c Reference 1; experimental rotational constants are 17236.6, 6002.9, and 4578.8 MHz for A, B, and C, respectively, for the normal species. ^d Reference 10. ^e Total of 22 independent parameters (12 for *cis*, 17 for *gauche*, including 7 overlapping) from MP2/6-311++G(d,p) structures are adjusted to fit all rotational constants of 19 isotopic species from ref 1. The maximum error for rotational constants is 0.06%.

TABLE 5: Comparison of Computed and Experimental Structural Parameters for *gauche*-3-Fluoropropene^a

parameter	MP2/6- 31G(d)	MP2/6- 31G(d,p) ^b	RHF/6- 311G(d,p)	MP2/6- 311G(d,p)	RHF/6- 311++G(d,p)	MP2/6- 311++G(d,p) ^c	r_s^d	r_0^e	microwave adjusted ^f
$r(C_1=C_2)$	1.336	1.335	1.3164	1.3373	1.3182	1.3393	1.354 ± 0.015	1.335 ± 0.003	1.334
$r(C_2-C_3)$	1.491	1.490	1.4956	1.4931	1.4958	1.4922	1.486 ± 0.015	1.490 ± 0.004	1.491
$r(C_3-F)$	1.401	1.399	1.3713	1.3911	1.3731	1.3987	1.371 ± 0.015	1.394 ± 0.004	1.400
$r(C_1-H_5)$	1.086	1.081	1.0775	1.0862	1.0775	1.0863	1.098 ± 0.015	1.086 ± 0.008	1.089
$r(C_1-H_6)$	1.084	1.079	1.0756	1.0842	1.0756	1.0844	1.054 ± 0.015	1.084 ± 0.006	1.087
$r(C_2-H_7)$	1.088	1.083	1.0782	1.0873	1.0783	1.0875	1.090 assumed	1.088 ± 0.020	1.091
$r(C_3-H_8)$	1.095	1.090	1.0841	1.0942	1.0840	1.0937	1.137 ± 0.020	1.095 ± 0.015	1.099
$r(C_3-H_9)$	1.095	1.091	1.0823	1.0934	1.0823	1.0930	1.127 ± 0.020	1.095 ± 0.008	1.098
$\angle C_1C_2C_3$	123.3	123.3	124.0	123.1	123.8	122.8	121.6 ± 1.0	123.3 ± 0.5	123.8
$\angle C_2C_3F$	109.6	109.6	109.9	110.1	110.0	109.9	110.9 ± 1.0	110.4 ± 0.5	109.6
$\angle C_2C_1H_5$	121.5	121.3	121.8	121.1	121.8	121.1	119.2 ± 1.0	121.5 (fixed)	119.7
$\angle C_2C_1H_6$	121.8	121.7	121.8	121.6	121.5	121.5	121.5 ± 1.0	121.8 (fixed)	120.5
$\angle H_5C_1H_6$	116.7	117.0	116.7	117.3	116.7	117.4	119.3 ± 1.0	116.7 (fixed)	119.8
$\angle C_1C_2H_7$	120.7	120.6	120.5	120.6	120.5	120.7	119.0 assumed	120.7 (fixed)	122.7
$\angle C_2C_3H_8$	111.5	111.0	110.9	110.9	111.1	111.4	107.4 ± 1.5	111.5 (fixed)	109.0
$\angle C_2C_3H_9$	111.2	111.5	111.4	110.7	111.6	111.1	105.2 ± 1.5	111.2 (fixed)	110.8
$\angle H_8C_3H_9$	108.9	109.4	109.3	109.3	109.3	109.5	111.4 ± 1.5	108.9 (fixed)	110.6
$\angle H_8C_3F$	107.1	107.3	107.0	107.2	106.8	106.8	107.1 ± 1.5	107.1 (fixed)	108.4
$\angle H_9C_3F$	108.4	108.5	108.1	108.4	108.0	107.9	114.7 ± 1.5	108.4 (fixed)	108.4
dihedral	127.2	126.0	128.6	125.8	126.7	123.4	127.1 ± 3.0	124.6 ± 0.5	125.7
angle, φ									
A 27720.35 ^c	27959		27496	27907	28630	27241	28036	27720.3	27714
B 4263.63 ^c	4255		4248	4260	4311	4267	4288	4263.8	4264
C 4131.98 ^c	4107		4112	4126	4166	4152	4149	4132.1	4132
$-(E + 215)$ (hartree)			0.978077	1.683802	0.983755	1.695406			

^a Bond lengths in angstroms; angles in degrees; rotational constants in MHz. ^b Reference 8. ^c Additional parameters: $\tau(H_5C_1C_2C_3) = -1.6$, $\tau(H_6C_1C_2H_5) = 179.8$, $\tau(H_7C_2C_1C_3) = 181.1$. ^d Reference 1; experimental rotational constants for the normal species are A = 27 720.4, B = 4263.6, and C = 4132.0 MHz. ^e Reference 10. ^f Additional parameters: $\tau(H_5C_1C_2C_3) = -3.5 \pm 1.9$, $\tau(H_6C_1C_2H_5) = 179.4 \pm 0.4$, $\tau(H_7C_2C_1C_3) = 180.7 \pm 0.3$.

frequency shifts compared with the frequencies of similar bands in the corresponding spectra in the gas phase. Also, small frequency shifts can be observed in different rare gas solutions (Figure 1).

Although the region near 3000 cm⁻¹ in liquid Ar contains a rather well-separated doublet, the presence of bands on both sides makes the band profile analysis difficult. At the higher temperature in both liquid Kr and Xe, the half-widths of the

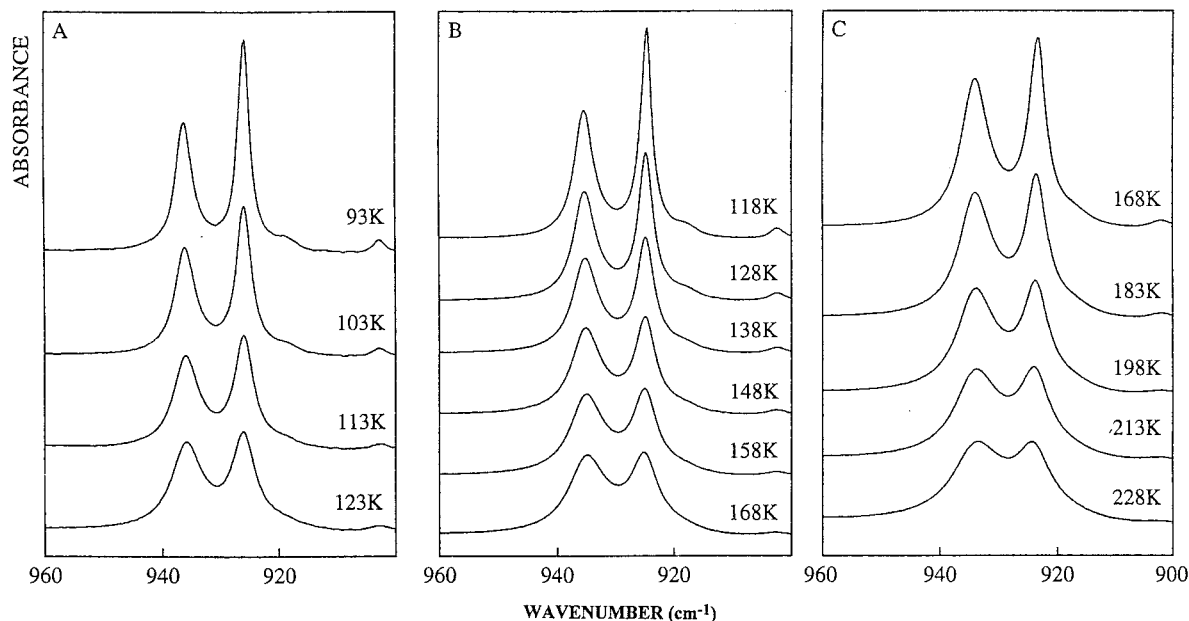


Figure 5. Temperature dependence of the infrared spectra in the region 950–900 cm^{-1} : (A) Ar; (B) Kr; (C) Xe.

bands prohibit a useful analysis. A similar remark must be made for the C=C stretching region where only at the lowest temperature in liquid Ar can a shoulder be clearly distinguished. Therefore, no band profile analysis has been performed for these regions. For the doublet at 1462/1470 cm^{-1} there is a shoulder near 1477 cm^{-1} , which causes problems in obtaining peak areas at higher temperatures. Similarly, for the 1430/1415 cm^{-1} doublet, a weak band on the low-frequency side of the high-frequency component causes difficulty in obtaining band areas. Therefore, the only doublet where little difficulty was encountered from nearby weak transitions is the one near 930 cm^{-1} .

The intensities of the conformational doublet, observed at 934 and 923 cm^{-1} (Figure 5) and assigned to the =CH₂ out-of-plane bend of the gauche and cis conformers, respectively, were obtained as a function of temperature and their ratio I_g/I_c measured. The curve-fitting procedure to obtain the areas under the bands has been used to obtain reliable intensity ratios. By application of the van't Hoff equation,

$$-\ln(I_g/I_c) = (\Delta H/(RT)) - \ln(\alpha_g/\alpha_c) - (\Delta S/R)$$

where ΔS is the entropy change and ΔH can be derived from the slope of a plot of $-\ln(I_g/I_c)$ versus $1/T$. It is assumed that ΔH , ΔS , and the quantity $\ln(\alpha_g/\alpha_c)$ are independent of the temperature over the experimental temperature range.

The van't Hoff plots are shown in Figure 6, and the plots are quite linear for the Kr and Ar solutions, whereas that for the Xe solution is not as linear. The ΔH values of 81 ± 1 , 72 ± 4 , and 60 ± 8 cm^{-1} have been determined from the Ar, Kr, and Xe solutions, respectively. These values are slightly higher than the value of 58 ± 23 cm^{-1} determined by Hirota¹ but considerably lower than the value of 263 ± 25 cm^{-1} , which was obtained from the variable temperature studies of the Raman spectrum of the vapor.⁴ The value is also much smaller than the value of 211 ± 25 cm^{-1} obtained from the infrared spectrum of the matrix-isolated material.⁸ It should be noted that all experimental results indicate that the cis conformer is the more stable form in all three physical states.

By use of a reaction field approximation, it has been shown that there is a linear relationship between the Kirkwood function $(\kappa - 1)/(2\kappa + 1)$ of the solvent and the enthalpy difference

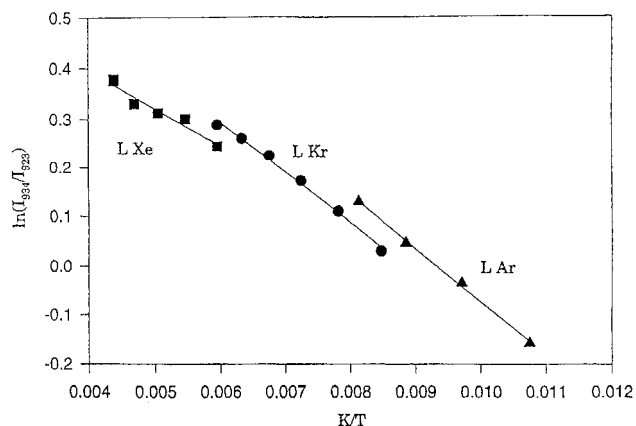


Figure 6. Plot of $-\ln(I_{934}/I_{923})$ vs $1000/T$.

measured in that solvent.^{25,26} This model has been applied to the allyl fluoride data obtained herein, and the graph resulting from this plot is shown in Figure 7. In this figure, also the least-squares straight line through the experimental points is given.

The linear regression of Figure 7 can be used to obtain a value for the enthalpy difference for the vapor phase. For the latter, the relative permittivity κ is approximated to be 1 so that the vapor-phase ΔH is obtained as the intercept of the straight line. It is clear from Figure 7 that this extrapolation must be carried out over a relatively large distance, but the high degree of linearity of the experimental points ensures that a reliable value for the vapor-phase enthalpy difference is obtained. The value of the intercept obtained is 130 ± 25 cm^{-1} , i.e., somewhere in the middle of the range of the available experimental values but lower than the ab initio values where the cis conformer is predicted to be the more stable form and lower than the Raman value for the vapor phase. We believe this is a reasonable value to use for the determination of the potential function parameters governing conformer interchange.

Torsional Potential Function

The computed energies for the conformational isomers of 3-fluoropropene from the various basis sets are collected in Table 6. From a comparison of the energy difference between

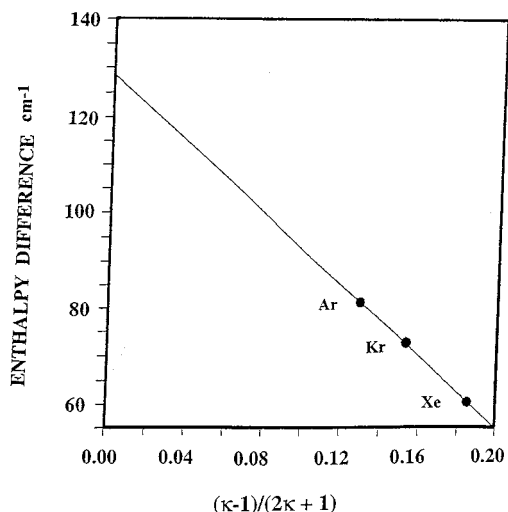


Figure 7. Enthalpy difference for the conformational equilibria of 3-fluoropropene as a function of the Kirkwood function. The experimental values for the different rare gas solutions are represented by the dots. The straight line is the result of the linear regression on the experimental points.

the conformers, one finds that these differences decrease with the increase in the basis set size and electron correlation. When the 6-311G(d,p) basis set was used, the enthalpy differences are determined to be 174 and 192 cm^{-1} at the RHF and MP2 levels, respectively, favoring the cis conformer as being the more stable rotamer. Furthermore, calculations at the RHF/6-311++G(d,p) level indicate that the energy separation reduces to 19 cm^{-1} . Surprisingly, with electron correlation with this basis set, the calculation reverses the energy ordering and predicts the gauche conformer to be more stable than the cis form (Table 6) by 117 cm^{-1} . The experimentally determined ΔH value clearly shows this prediction to be in error. It is probable that the MP2/6-311G(d,p) calculation gives better energy differences between the conformers whereas the MP2/6-311++G(d,p) calculation gives better structural parameters.

On the basis of our ab initio values, the torsional potential energy curve can be constructed by a best-fit Fourier cosine series as a function of torsional angle:

$$V(\phi) = \frac{1}{2} \sum_{i=1}^6 V_i (1 - \cos i\phi)$$

The calculated potential curves at various levels of theory are depicted in Figure 8. The potential coefficients and barriers governing internal rotation of the $-\text{CH}_2\text{F}$ moiety against a molecular frame are summarized in Table 6. The ab initio predictions, with the exception of the MP2/6-311++G(d,p) calculation, give results that are in reasonable agreement with the experimental results regarding the existence and relative stabilities of the cis and gauche conformers. Moreover, the predominance of the calculations indicates that the cis conformer is the thermodynamically preferred rotamer.

Vibrational Analysis

To obtain a more complete description of the molecular motions involved in the fundamental modes of this molecule, a normal coordinate analysis was carried out. This analysis was performed utilizing ab initio calculations and the Wilson GF matrix method.¹⁶ The Cartesian coordinates taken from the

optimized structure were input into the B matrix program together with the complete set of 24 internal coordinates (Figure 2). This set of internal coordinates was used to form the symmetry coordinates with three redundancies.⁶ The symmetry coordinates were used to determine the corresponding potential energy distributions (PED). The resulting B matrix converts the ab initio force field in Cartesian coordinates to a force field in the desired internal coordinate. Finally, scaling factors of 0.9 for the stretching and bending modes, 1.0 for torsions, and the geometric average of scaling factors for the interaction force constants were used to obtain the fixed scaled force field and resultant frequencies, along with the potential energy distributions (PED), which are summarized in Tables 2 and 3.

The predicted vibrational fundamentals obtained from the MP2/6-311G(d,p) and MP2/6-311++G(d,p) calculations give almost the same wavenumbers, and for most modes, the differences are less than 10 cm^{-1} . The assignments given in Tables 2 and 3 have been made on the basis of the characteristic group and calculated frequencies, the ab initio predicted intensities for the infrared and Raman spectra, along with support from changes in relative intensities of doublets obtained from temperature-dependent infrared spectra of the rare gas solutions.

There is a problem in the assignment of the carbon–hydrogen, $-\text{CH}_2(\text{F})$, antisymmetric and symmetric stretches for the cis conformer, since there are three bands at 2888, 2943, and 2963 cm^{-1} in the Raman spectrum of the solid with similar bands in the corresponding infrared spectrum. Clearly, one of these bands is due to Fermi resonance, but it is not clear whether the doublet is the 2888/2943 cm^{-1} bands or the 2943/2963 cm^{-1} bands. In our earlier study⁵ we chose the 2888/2943 cm^{-1} bands as the Fermi doublet with the assumption that it was due to the overtone of the CH_2 deformation (1455 cm^{-1}). Therefore, the CH_2 symmetric stretch was assigned to the 2943 cm^{-1} Raman line, since this is the strongest Raman line of the three under consideration. This assignment is consistent with the predictions of the intensity of this line from the ab initio calculations. The CH_2 antisymmetric stretch is then assigned to the 2963 cm^{-1} band, which is in agreement with ab initio predictions as well as with earlier proposed vibrational assignments.^{5,8}

Another area where the assignments are questionable is the region from 900 to 1100 cm^{-1} . The ab initio calculations indicate that the band near 1100 cm^{-1} is the C–F stretch for the cis conformer, which should give rise to a very strong infrared band as found at 1118 cm^{-1} . The corresponding gauche mode in this region (1160 cm^{-1}) is a very mixed mode with the major contribution (25%) from the C–C stretch, which leaves the band at 1099 cm^{-1} as a combination or overtone mode. The remaining bands in this region, which are mostly doublets, were assigned on the basis of their relative changes in intensity with changes in temperature of the rare gas solutions.

The low-frequency skeletal deformations, i.e., the C=C–C and C–C–F bending modes, involve four heavy atoms with nearly equal atomic weight. This results in a high degree of mixing of these skeleton vibrational modes. An interesting feature is that the higher frequency band at 604 cm^{-1} for the cis rotamer is more CCF bend at 44% compared to 31% for the CCC bend, whereas for the gauche conformer the higher frequency mode at 422 cm^{-1} is 51% CCC bend and only 20% CCF bend. The lower frequency bend at 332 cm^{-1} for the gauche rotamer is made up of 49% CCF bend and 32% CCC bend. Part of this difference is due to the lower symmetry of the gauche conformer, which results, in general, in a significant increase in the mixing of the modes.

TABLE 6: Barriers to Internal Rotation (cm⁻¹), Enthalpy Difference (cm⁻¹), and Dihedral Angles (deg) for 3-Fluoropropene^a

parameter	MP2/6-31G(d,p) ^a	RHF/6-311G(d,p) ^b	MP2/6-311G(d,p) ^b	RHF/6-311++G(d,p) ^b	MP2/6-311++G(d,p) ^b	ref 6	this study ^c
V ₁	20.9	-153.0	-15.1	-263.9	-174.6	36 ± 9	-162 ± 9
V ₂	325.6	390.4	242.0	266.8	15.1	296 ± 10	333 ± 12
V ₃	841.0	885.3	839.9	893.7	800.9	826 ± 15	860 ± 5
V ₄	3.7	17.0	15.2	28.0	-26.4	47 ± 7	65 ± 2
V ₅	5.7	28.5	37.8	26.3	17.7	14 ± 8	-13 ± 5
V ₆	-7.4	-45.4	-56.1	-42.5	-45.7	-32 ± 5	-35 ± 2
cis-to-gauche barrier	1103	1162	1038	1055	759	1098	1117
gauche-to-gauche barrier	612	585	670	636	769	588	526
gauche-to-cis barrier	847	988	846	1036	876	810	958
energy (enthalpy) difference	256	174	192	19	-117	263 ± 25	130 ± 25
torsional dihedral angle (gauche)	126.0	128.6	125.8	126.7	123.1	124.3 ± 0.5	124.6

^a Data taken from refs 8 and 16. ^b This study. ^c Calculated from the observed far-infrared transitions (Table 8) and the following kinetic terms: $F_0 = 2.65251$, $F_1 = 0.51078$, $F_2 = 0.22400$, $F_3 = 0.05046$, $F_4 = 0.01501$, $F_5 = 0.00386$, $F_6 = 0.00109$, $F_7 = 0.00031$, and $F_8 = 0.00008$ cm⁻¹.

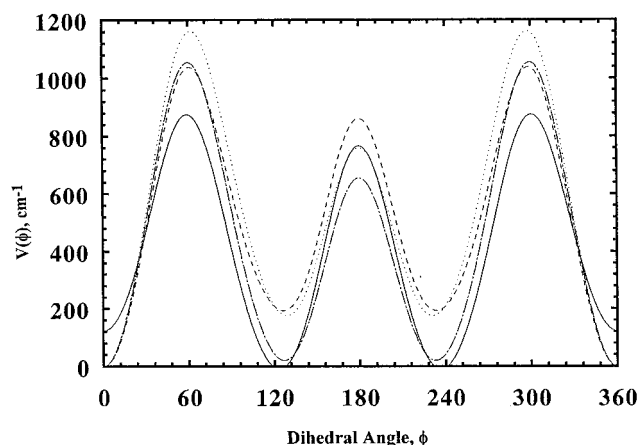


Figure 8. Potential function governing the internal rotation around the C–C bond determined by ab initio calculations: MP2/6-311++G(d,p); MP2-6-311G(d,p); RHF/6-311++G(d,p); RHF/6-311G(d,p).

Discussion

On the basis of the fact that the calculated structural parameters with the larger basis sets with electron correlation are in excellent agreement with the experimentally determined r_o parameters clearly indicates that the ab initio calculations with such basis sets can be used to obtain the structural parameters for these types of molecules. The major difference in the structural parameters, in addition to the two CCC and CCF angles between the gauche and cis conformers, is the C–F distance. We have attempted to fit the microwave rotational data by maintaining the difference between the C–F distances that were predicted from the ab initio calculations, and the results are very satisfactory.

A new computer program, AandM (ab initio and microwave), has been developed. This program combines the information from microwave and ab initio calculations and gives structural parameters that fit the rotational constants with the structural parameters remaining close to the ab initio values. To reduce the number of independent variables, the structural parameters are separated into several sets according to their type. For example, three CH bond lengths may form one set and three CCH angles may form another set. Each set uses only one independent parameter in the optimization, and all structural parameters in one set will be adjusted by the same parameter, i.e., an adjustment factor. The information on the differences between the similar parameters from ab initio calculations will be retained in the final results by the following method: bond lengths in the same set will keep their relative ratio and bond

angles and torsional angles in the same set will keep their differences in degrees. If one CH bond is 1% longer than another CH bond by ab initio calculation, it will still be 1% longer after the optimization. If a CCH angle is 1° larger than another CCH angle from the ab initio calculation, it will still be 1° larger in the final result. This assumption is based on the fact that the errors from ab initio calculations are systematic, which is now commonly accepted, and this technique is currently used in our normal coordinate analysis. The program searches the minima of the function $F(k_1, k_2, \dots)$:

$$F(k_1, k_2, \dots) = \sum_i (100K_i)^2 + \sum_j (20K_j)^2 + \sum_l (0.1K_l)^2 + \sum_m (0.02K_m)^2$$

The adjustment factors K in the formula above are defined as

$$K_i = \frac{R_{ci} - R_{oi}}{R_{oi}}$$

$$K_j = \frac{L_{cj} - L_{aj}}{L_{aj}}$$

$$K_l = A_{cl} - A_{al}$$

$$K_m = T_{cm} - T_{am}$$

where R , L , A , and T represent the rotational constants, bond lengths, bond angles, and torsional angles, respectively. The lower case letters c , o , and a indicate calculated (calculated here means calculated by the AandM program, not by the ab initio program), observed (rotational constants), and ab initio (bond lengths) bond angles and torsional angles in degrees. Thus, the symbols T_c and T_a indicate the torsional angles calculated from the program and the torsional angles obtained from the ab initio predictions, respectively. The subscript runs over all structural parameters in the optimization. The real meaning of these formulas is the following: 1% error of any rotational constant contributes 1.0 to the function F , which is equivalent to a 5% shift of a bond length from its ab initio value, a 10° shift of bond angle from its ab initio value, or a 50° shift of a torsional angle from its ab initio value. Only real torsional angles around single bonds are considered as torsional angles in the calculations, whereas other angles defined by the third internal coordinate in the ab initio input data are treated as bond angles because they are not as flexible as real torsion angles around

single bonds. To avoid the possibility of falling into a local minimum instead of the global minimum of F , the simplex algorithm instead of the gradient method was used to optimize the adjustment factors in searching for the minimum of F .

This program adds ab initio structural parameters, although with much smaller weights, to the rotational constants so that the number of observables is always larger than the number of unknown parameters. As a consequence, we can obtain unique results without any arbitrary assumptions for the values of structural parameters.

The structural parameters are grouped in this way: all CH bond lengths in the ethylene group are grouped into one set and the other two CH bond lengths in the molecule are in another set. Two HCCF dihedral angles (not in ethylene group) are grouped together. Additionally, sets of structural parameters in two conformers are combined further to reduce the number of independent parameters. Corresponding sets of bond lengths as well as two C=CH angles in the two conformers are combined. The reasons for combining the parameters in this way are that the errors of ab initio calculations in bond lengths are smaller and more systematic than in bond angles and that the angles of the ethylene group are more stable than the other angles. The C=CH angles in the position cis to the CC single bond in the two conformers are not combined because this H atom is more affected by the CF bond in the cis conformer. Therefore, the independent parameters are reduced to the number 22, which is much less than the number of available rotational constants of 11 isotopic species in the optimization. The final fitting of the rotational constants is satisfactory with maximum relative and absolute errors no more than 0.06% and 7.8 MHz, respectively (Table VIII in Supporting Information). These structural parameter results are listed in the last columns of Tables 4 and 5 as microwave-adjusted parameters. It is difficult to estimate the uncertainties in these structural parameters, but they should be less than those obtained as r_o parameters from just the microwave rotational constants in the previous determination.

The ab initio calculations indicate that the C–F bond distance should be 0.01 Å shorter in the cis conformer compared to that found in the gauche rotamer. By use of this difference as well as the predicted difference of the other parameters, it was possible to fit all of the previously determined rotational constants and obtain reasonable structural parameters without fixing any of them. The previously reported¹⁰ r_o parameters are the same within the given uncertainty. However, it was not necessary to fix any of the angle parameters for the gauche conformer. It is readily apparent that many of the previously reported¹ r_s parameters for the gauche form were in error (Table 5) whereas most of the r_s parameters for the cis conformer were satisfactory except for the C–H₆, which is much too long (Table 4). Parameters obtained by this method should be closer to the actual parameters than those obtained by holding some parameters fixed while obtaining the other from the microwave rotational constants. This procedure should be useful for obtaining structural parameters for many other molecules where the number of rotational constants is significantly smaller than the number of structural parameters in the molecule.

The value of ΔH has been determined rather accurately via the cryosolution method in three different rare gas solutions, which indicates that the cis form is more stable than the gauche rotamer. We have extrapolated these data to the vapor and obtained an enthalpy value of $130 \pm 25 \text{ cm}^{-1}$. This is much higher than the value of $58 \pm 10 \text{ cm}^{-1}$ obtained from the Raman spectrum of the liquid;⁵ however, it is significantly lower than

the value of $263 \pm 23 \text{ cm}^{-1}$ by a variable-temperature-dependent experiment of the Raman spectrum of the vapor.⁴ The lower value of 58 cm^{-1} for the liquid is attributed to dipole–dipole interactions in this phase, whereas the larger value of $263 \pm 23 \text{ cm}^{-1}$ determined from the gas probably reflects the experimental uncertainties arising from intensity measurements in the vapor by the Raman technique. First, there is the problem of measuring the temperature of the gas where the cell must be hotter on the side where the hot nitrogen gas initially contacts the cell compared to the other side. Also, intensity measurements are difficult to make for the Raman spectrum and, additionally, the heights of the bands were previously used rather than areas under the curve. Finally, it should be noted that there is another fundamental at 928 cm^{-1} for the cis conformer that is close to the 920 cm^{-1} band used for the ΔH measurement of the Raman spectrum of the vapor. Although the 928 cm^{-1} line is an A'' mode, which will not have a Q branch in the Raman spectrum, it will have very broad R, S, P, and O branches that could contribute to the intensity of the 920 cm^{-1} Q branch of the A' mode. In our present determination, the conformational pairs utilized are well separated with reasonable intensities and, by using the curve fitting procedure, the intensity ratios at different temperatures can be determined with high accuracy. Additionally, the temperature of the sample is accurately measured, and therefore, the ΔH obtained in this study can be considered as more reliable than those previously reported.

Spectroscopic evidence on the conformational stability can also be found by a comparison of the calculated Raman spectrum of the mixture with the previously reported experimental spectrum.^{4,5} They closely match in both band positions and intensities. By review of these theoretical and experimental spectra, the conclusion can be drawn confidently that the cis conformer is the thermodynamically preferred conformer with an enthalpy difference of $\sim 100 \text{ cm}^{-1}$.

The simulated infrared spectrum closely resembles the observed spectrum, which provides excellent evidence for the quality of the ab initio calculations. The calculated frequencies agree within about 1% of those obtained from the cryosolution as well as with those obtained from the matrix isolation spectroscopic results performed by Nieminen et al.⁸ Because a significant number of vibrational modes of this molecule involve extensive mixing, it results in some difficulties in the assignments of the normal modes. Under the guidance of the normal coordinate analysis, along with the relative intensities of the doublets with changes of temperature of the rare gas solutions, we believe correct assignments have been made for the fundamentals for both conformers. As pointed out in the previous study,⁴ there is some difficulty in ascertaining the torsional fundamental for the gauche conformer (108.05 or 92.10 cm^{-1}). Our calculation for the gauche conformer closely matches the experimental results, which are based on the $1\bar{7} \leftarrow 0\pm$ transition originating at 108.05 cm^{-1} . Therefore, the calculated 114 cm^{-1} value for this mode seems to add support for the assignment to the higher frequency band and leaves unexplained why the prediction¹ of $84.6 \pm 2.8 \text{ cm}^{-1}$ from the microwave data has such a large error. An error of nearly 30% is much larger than expected where frequently predictions better than 10% have been made by this technique. Therefore, it would be of interest to repeat these measurements to see if, in fact, they are in error or if the gauche torsional fundamental should be assigned to the lower frequency band.

With the more accurate ΔH value, as well as more accurate structural parameters, we have recalculated the potential function governing the conformational interchange. We have used the

TABLE 7: Torsional Transitions (cm^{-1}) and Assignment of Gaseous 3-Fluoropropene

conformer	transition	observed	calculated ^a	Δ
cis	1 \leftarrow 0	164.41	164.36	0.05
	2 \leftarrow 1	157.69	158.11	-0.42
	3 \leftarrow 2	151.392	150.91	0.49
	4 \leftarrow 3	142.57	143.50	1.32
gauche	1 \mp \leftarrow 0 \pm	108.05	108.05	0.00
	2 \mp \leftarrow 1 \pm	104.55	104.38	0.28
	3 \mp \leftarrow 2 \pm	99.62	99.38	-0.13
	99.75	0.24		

^a Calculated with the six-parameter potential function listed in Table 4.

dihedral angle obtained from the fit of the microwave data for the gauche conformer to eliminate the strong correlation of the V_1 and V_2 terms in the potential function. The fit of the torsional fundamentals for the two conformers and the associated "hot bands" is given in Table 7. The determined potential parameters are listed in Table 4 and compared to those obtained in previous studies of 3-fluoropropene, as well as those obtained from the various ab initio calculations. Because of the much lower value for ΔH , the V_1 term is now negative ($-162 \pm 9 \text{ cm}^{-1}$), whereas it was previously reported as positive ($36 \pm 9 \text{ cm}^{-1}$). The negative value is consistent with the value of this parameter from the ab initio calculations. The other parameters are very similar to those previously obtained except for the V_5 term, which now has a small negative value ($-13 \pm 5 \text{ cm}^{-1}$), whereas it was previously reported as positive ($14 \pm 8 \text{ cm}^{-1}$) from the previously reported potential function governing the conformational interchange.

It is interesting to compare the enthalpy difference between the two stable conformers when the hydrogen on the carbon 2-position is replaced by a methyl group or a chlorine atom. With the substitution of the chlorine atom at the 2-position there is stabilization of the cis conformer that is predicted by the ab initio calculations.²⁷ On the other hand, substitution of a methyl group at the 2-position favors the gauche conformer, and the ab initio calculations indicate that the two conformers have nearly equal energies.²⁸ The preliminary results for the molecule substituted with a methyl group on the 1-position indicate that the gauche conformer is favored. It would be interesting to see if the ab initio calculations predict this trend for this molecule, and we plan to carry out such calculations in the near future.

In general, the theoretical calculations with a relatively large basis set at the MP2 level can provide accurate geometric parameters and reasonable guidance for the vibrational assignment. However, as shown in the present study, when calculating the energy difference between molecular conformers with values less than 1.0 kcal/mol, caution must be used on utilizing the conformer stability information. At this time the results need to be verified by an experimental investigation.²⁹

Acknowledgment. W.A.H. thanks the Fund for Scientific Research (FWO, Belgium) for successive appointments as a Research Assistant and Postdoctoral Fellow. The FWO is also thanked for financial help toward the purchase of the spectro-

scopic equipment utilized in this study. J.R.D. acknowledges partial support of these studies by the University of Missouri–Kansas City Faculty Research Grant program. The authors also acknowledge NATO for a travel grant, which made it possible to complete this study.

Supporting Information Available: Table VIII listing the fit of the rotational constants (MHz) of cis and gauche 3-fluoropropene microwave-adjusted structural parameters (r_o). This material is available free of charge via the Internet at <http://pubs.acs.org>.

References and Notes

- (1) Hirota, E. *J. Chem. Phys.* **1965**, *42*, 2071.
- (2) Meakin, P.; Harris, D. D.; Hirota, E. *J. Chem. Phys.* **1969**, *51*, 3775.
- (3) McLachlan, R. D.; Nyquist, R. A. *Spectrochim. Acta* **1968**, *24A*, 103.
- (4) Durig, J. R.; Zhen, M.; Little, T. S. *J. Chem. Phys.* **1984**, *81*, 4259.
- (5) Durig, J. R.; Zhen, M.; Heusel, H. L.; Joseph, P. J.; Groner, P.; Little, T. S. *J. Phys. Chem.* **1985**, *89*, 2877.
- (6) Durig, J. R.; Geyer, T. J.; Little, T. S.; Durig, D. T. *J. Mol. Struct.* **1988**, *172*, 165.
- (7) Santhanam, V.; Sobhanadri, J.; Subramaniam, S. *Pramana* **1988**, *30*, 51.
- (8) Nieminen, J.; Murto, J.; Rasanen, M. *Spectrochim. Acta* **1991**, *47A*, 1495.
- (9) Durig, J. R.; Lee, M. J.; Badawi, H. M.; Sullivan, J. F.; Durig, D. T. *J. Mol. Struct.* **1992**, *266*, 59.
- (10) Durig, D. T.; Little, T. S.; Costner, T. G.; Durig, J. R. *J. Mol. Struct.* **1992**, *266*, 277.
- (11) Bulanin, M. O. *J. Mol. Struct.* **1995**, *347*, 73.
- (12) Moller, C.; Plesset, M. S. *Phys. Rev.* **1934**, *46*, 618.
- (13) Hoffman, F. W. *J. Org. Chem.* **1949**, *14*, 105.
- (14) Frisch, M. J.; Trucks, G. W.; Schlegel, H. B.; Gill, P. M. W.; Johnson, B. G.; Robb, M. A.; Cheeseman, J. R.; Keith, T. A.; Petersson, G. A.; Montgomery, J. A.; Raghavachari, K.; Al-Laham, M. A.; Zakrzewski, V. G.; Ortiz, J. V.; Foresman, J. B.; Cioslowski, J.; Stefanov, B. B.; Nanayakkara, A.; Challacombe, M.; Peng, C. Y.; Ayala, P. Y.; Chen, W.; Wong, M. W.; Andres, J. L.; Replogle, E. S.; Gomperts, R.; Martin, R. L.; Fox, D. J.; Binkley, J. S.; Defrees, D. J.; Baker, J.; Stewart, J. P.; Head-Gordon, M.; Gonzalez, C.; Pople, J. A. *Gaussian 94*, revision B.3; Gaussian Inc.: Pittsburgh, PA, 1995.
- (15) Pulay, P. *J. Mol. Phys.* **1969**, *17*, 197.
- (16) Luppi, J.; Rasanen, M.; Murto, J.; Pajunen, P. *J. Mol. Struct.* **1991**, *245*, 307.
- (17) Wilson, E. B.; Decius, J. C.; Cross, P. C. *Molecular Vibrations*; McGraw-Hill: New York, 1955.
- (18) Frisch, M. J.; Yamaguchi, Y.; Gaw, J. F.; Schaefer, H. F., III; Binkley, J. S. *J. Chem. Phys.* **1986**, *84*, 531.
- (19) Amos, R. D. *Chem. Phys. Lett.* **1986**, *124*, 376.
- (20) Chantry, G. W. In *The Raman Effect*; Anderson, A., Ed.; Marcel Dekker Inc.: New York, 1971; Vol. 1, Chapter 2.
- (21) Polavarapu, P. L. *J. Phys. Chem.* **1990**, *94*, 8106.
- (22) Bulanin, M. O. *J. Mol. Struct.* **1973**, *19*, 59.
- (23) van der Veken, B. J.; DeMunck, F. R. *J. Chem. Phys.* **1992**, *97*, 3060.
- (24) Herrebout, W. A.; van der Veken, B. J.; Wang, A.; Durig, J. R. *J. Phys. Chem.* **1995**, *99*, 578.
- (25) Herrebout, W. A.; van der Veken, B. J. *J. Phys. Chem.* **1996**, *100*, 9671.
- (26) Wong, M. W.; Frisch, M. J.; Wiberg, K. B. *J. Am. Chem. Soc.* **1991**, *113*, 4776.
- (27) Durig, D. T.; Guirgis, G. A.; Durig, J. R. *Struct. Chem.* **1992**, *3*, 347.
- (28) Durig, J. R.; Qui, H. Z.; Durig, D. T.; Zhen, M.; Little, T. S. *J. Phys. Chem.* **1991**, *95*, 2745.
- (29) Mack, H. G.; Oberhammer, H. *J. Mol. Struct.: THEOCHEM* **1992**, *258*, 197.